

DAMAGING AND EJECTION PROCESSES DURING HVI ON BRITTLE TARGETS: EXPERIMENTAL DATA AND COMPARISON WITH NUMERICAL SIMULATION USING AN SPH METHOD

Y. Michel^(1, 2, 3), A. Moussi^(1, 4), C. Durin⁽¹⁾, C. Espinosa⁽³⁾, J.M. Chevalier⁽²⁾, J.C. Mandeville⁽⁴⁾

⁽¹⁾CNES- BP 4025, 18 avenue Edouard Belin F-31055 Toulouse Cedex

⁽²⁾CEA-CESTA /DEV/SDET/LDDT - BP 2, F-33114 Le Barp

⁽³⁾ENSICA - 1 Place Emile Blouin, F-31056 Toulouse Cedex 54. Contact : yann.michel@ensica.fr

⁽⁴⁾ONERA-CERT-DESP - BP 4025, 2 avenue Edouard Belin F-31055 Toulouse Cedex

ABSTRACT

Hypervelocity impacts on a spacecraft's surfaces result in ejecta or secondary debris production. These ejecta may contribute to a modification of the debris environment. Brittle materials are particularly sensitive to hypervelocity impacts and produce features larger than those observed on ductile targets. CEA faces to the same problem in the Laser MégaJoule project (LMJ), optics of large lasers are exposed to the chamber environment including hypervelocity shrapnel. This paper is devoted to the damaging and ejection processes during hypervelocity impacts on thin brittle targets (2mm thick fused silica targets for 500_μm steel projectiles). Numerical simulations using Ls-Dyna SPH method and the JH2 material model were compared to experimental data obtained with CEA's light gas gun with satisfying results. Fragments ejected during the impact were experimentally collected, analysed and compared to the calculations.

1. INTRODUCTION: COMMON INTERESTS OF CNES-ONERA AND CEA ON HVI INVOLVING BRITTLE TARGETS

The increasing willing of space companies to reduce spacecrafts cost has, in recent years, led to the development of satellites with longer operational lifetime. Increasing the longevity of satellites presents many constraints in terms of material degradation due to the space environment and many satellites undergo anomalies during their operating life. The meteoroids and debris environment play an important role in the reduction of spacecraft life time. Ejecta or secondary debris, are produced when a debris or a meteoroid impact a spacecraft surface. Three different ejection processes can be identified and are presented in figure 1: jetting (fast liquid particles ejected at grazing angles), cone (small and fast particles ejected at angles depending on the impact conditions), spall fragments (large fragments ejected at low velocities).

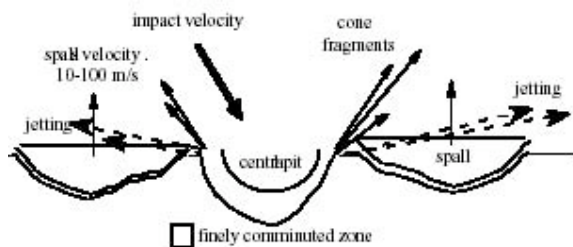


Figure 1 Ejecta mechanisms: jetting, cone and spalls

1.1. Role of brittle materials in space debris proliferation

Among many materials used on satellites, brittle materials are particularly sensitive to hypervelocity impacts because they are essential within the mission (they are used for optics or solar cells) and because they represent very large surfaces exposed to the debris and meteoroids environment. Moreover, as it has been highlighted by large solar arrays returned from the Eureka Mission and Hubble Space Telescope, hypervelocity impact on brittle materials produce features not observed on ductile targets. Low fracture toughness and high yield strength produce a range of morphologies including cracking, spallation and shatter. Impact features are typically characterised by petaloid spallation separated by radial cracks which extend to much larger volumes than the primary crater and subsequently remove most or all of the primary crater, especially for thin targets. Thus, because of both large surface exposure and large damaged volume, a great number of fragments are ejected at high velocities and brittle materials play a very important role in the potential degradation of the space environment. As it has been reported by Bariteau and Mandeville (2001), the ejected volume can be 100 times higher than the impacting volume in the case of brittle targets and some spalls are much bigger than the particle. This underlines the importance of understanding the damaging and ejection processes for a better comprehension of modifications of the debris environment on earth orbits. Some recent evolutions of the debris and micrometeoroids population reported by Moussi et al (2005) after analysis of Hubble solar arrays retrieved in 2002 underline the danger of this auto generation phenomenon. Figure 2 illustrates an increase in the total cumulative objects flux since 1993 which highlights an important raise of objects between 15 and 100 microns in diameter. This rise is mainly due to space debris but has to be normalised by the solar activity during the two periods. Indeed, the mean atmospheric density decreased from 1993 till 2002 so further studies are leading in order to determine if the population is only stabilised or increasing. According to the size range of these objects, it is probably due to secondary debris such as spalls. As the life time of such fragments does not exceed 10 days to a year, the secondary debris generation process needs to be much important to stabilise or increase the debris population. This observation underlines the interest to improve

knowledge of the ejecta phenomenon and capabilities to model material ejection occurring during hypervelocity impacts on thin brittle targets.

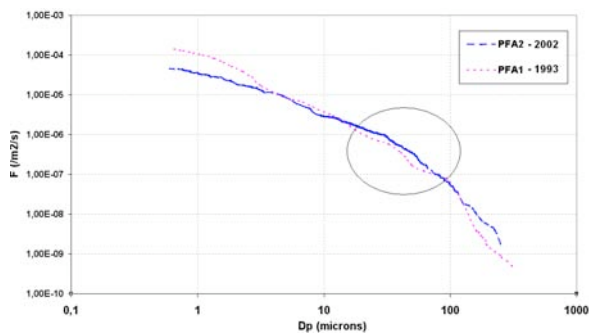


Figure 2 Increase in objects cumulative fluxes observed in 1993 and 2002. The fluxes are calculated from HST solar arrays retrieved from space in 1993 and 2002 (Moussi et al, 2005).

1.2. Environmental conditions of the Mega Joule Laser (LMJ) experiment chamber

The LMJ is one of the large experimental facilities of the Simulation program designed to avoid nuclear testing. The high-powered laser will be built at the CEA-CESTA facility (study centre under the Atomic Energy Commission's Military Applications Directorate). Its 240 beams will focus 1.8 megajoules of energy on a target placed in a vacuum at the centre of an test chamber. The various instruments used in the experiment chamber will undergo many aggressions resulting from target disassembly. Thus the large lasers optics will be bombarded by X-rays, neutrons, ions as well as debris and shrapnel. In this study, the authors will only focus potential impacts of debris and shrapnel on fused silica optical debris shields.

These Main Debris Shields called MDS are 20mm thick fused silica plates placed in front of each of the 240 lasers way out. 2 mm thick Disposable Debris Shields, DDS, located in front (with incidence) of the MDS might be used to stop vapour, particulate, droplets and substantially reduce very small shrapnel cratering on the main debris shields. But ejecta from the rear surface of the DDS and penetration through the DDS are likely to damage the MDS and seed new laser damage sites. The MDS lifetime is limited by the laser damage growth of those damage sites.

As it has been presented above, CEA is concerned by damages caused by hypervelocity impacts on thick brittle targets (20 mm thick Main Debris Shields) and on thin brittle target (DDS) located in front of these MDS. As fragments generated during an LMJ shot can perforate the DDS plate and/or generate secondary fragments that may impact MDS or will simply pollute the experiment chamber, CEA is also concerned by secondary debris generation as well as CNES is concerned by spalls and ejecta ejection in the space environment. To lead this study, CEA-CESTA has built a two stages light gas gun called MICA able to launch 2 mm projectiles at 5 km/s. All the MDS and the DDS presented in this article where impacted by MICA with either steel or glass projectiles. The following part presents the results of fused silica MDS/DDS post impact analysis (CEA-CESTA) as well as micro

impacts performed by ONERA-CERT and CNES semi infinite fused silica target for various projectiles.

2. ANALYSIS OF IMPACTED SAMPLES

Studying HVI effects on brittle material requires the establishment of an important database of impacted samples. CNES, ONERA, CEA and ENSICA have been working together for a couple of years to collect as many information as possible. This part presents briefly the different cases that have been simulated and/or analysed in the concerned laboratories first for brittle semi infinite then for thin targets.

2.1. Semi infinite brittle targets

The authors regard as important to present some of the results obtained with semi-infinite targets. Two main sources of data are concerned: semi-infinite pure silica targets impacted by ONERA and analysed at CNES, and main debris shields impacted at CEA-CESTA analysed by ENSICA.

The first sample family concerns 2mm thick fused silica disks impacted by 0.7-1.3_m iron spherical projectiles at velocities ranging from 2 to 12 km/s with several incidence angles (0°, 30°, 45° and 60°). The shooting campaign was performed with the electrostatic particle accelerator of the Max Planck Institute (Heidelberg). Figure 3 illustrates damage morphologies observed on silica involving very small projectiles at hyper velocities. Damages mainly consist of a central pit showing evidence of melted Fe residue droplets and a large spallation surface whose ellipticity depends on incidence angle (Moussi and Mandeville, 2005).



Figure 3 Normal HVI of iron dust on glass. On the right, a picture of the pit observed on glass at very high velocities showing evidence of Fe residue droplets

The second sample family concerns MDS plates impacted at CEA by MICA. MDS are 20mm thick fused silica plates. They were impacted by 500µm glass or steel projectiles at velocities ranging from 0.5 to 5 km/s. High velocity damage in SiO₂ MDS results in front side craters with large diameter relative to crater depth and internal flaws. These craters have circular pattern contours in outer regions; these patterns result from both internal cracks and surface spallation. A center area of heavier damage has also been observed and appears white on front-lit views (cf. figure 4). This area consists of a central pit showing the footprint of the projectile and a shattered zone at the periphery of the pit. The shattered zone is probably due to SiO₂ fragmentation and compaction during the shock loading as reported by Cagnoux (1985). No evidence of projectile residue was found on MDS samples for both glass and steel projectiles. Figures 4 and 5 illustrate observations made above. In some high energy cases, rear spallation without material ejection was observed on MDS. Adding this to the large damaged area and its potential effects on laser fluence incited CEA to investigate MDS

protection with thin DDS. DDS damage will be the object of part 2.2.

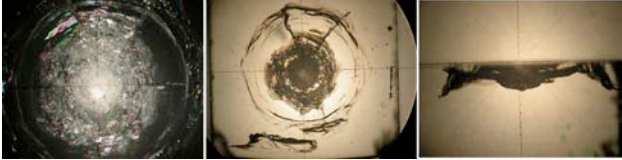


Figure 4 Damages observation caused by a HVI on a MDS at 2745 m/s. The left view is a front-lit view and shows the compaction area, the middle and right picture are back-lit view internal sample's damages

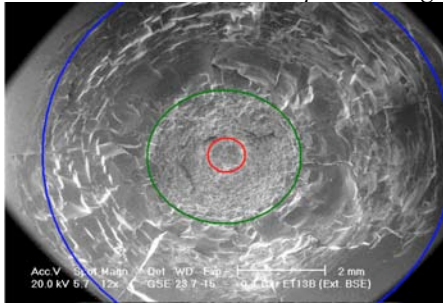


Figure 5 SEM view of a MDS impacted at 2745 m/s by MICA. The picture shows the different damages zone: the central pit, the compacted zone and the spall zone.

Even if CEA-CESTA and CNES-ONERA projects concern different scales (projectile sizes at velocities), the results presented above show many common points in terms of qualitative and quantitative damages and as consequence in terms of phenomenology that is: cracks and crater and ejecta arising from front spalls.

2.2. Thin brittle targets

The case of thin brittle targets is particularly interesting for two main reasons. First of all, as it has been presented earlier, solar cells which behave like thin brittle targets are the constitutive elements of solar arrays and they represent at the same time very large surfaces exposed to the space environment and a source of secondary debris. The second reason is related to the quantity of ejected matter during hypervelocity impact. Spall phenomenon is indeed the main source of ejection for any brittle target; further more spallation occurs at the front face and rear face of the sample even if there is no perforation. This characteristic is particularly important for HST solar cells for which the ejected volume during rear impact can be as much as hundred times higher than the impacting particle volume, as reported after HST-CS analysis performed at CNES.

The case of DDS designed to be used in the LMJ experiment chamber illustrates perfectly potential problems and danger caused by thin brittle targets: the question which should be raised consists in knowing if we will not generate more fragments while trying to protect the MDS. If cost effective DDS are necessary to protect MDS, what is the best configuration in terms of incidence and distance between DDS and MDS to avoid seeding to much damage in the MDS. To answer this, MICA shot campaign has been started in 2004 to study damages caused by HVI in DDS and potential damages caused by rear face matter ejection on MDS. Many 2mm thick DDS were impacted by glass and steel projectiles ($\varnothing=500\mu\text{m}$) for velocities ranging from 1000m/s to 3500m/s. As for thick targets, damages consist of three main characteristics: a perforation hole ($D_h \approx 2\text{mm}$) or a central pit, a shattered zone (also called

compacted zone) and a wide spallation zone. What was new on thin target is that these characteristics were observed for both front and rear faces. In all cases, the spallation zone on the rear face ($D_{\text{Spall Back}} \approx 7\text{-}10\text{mm}$) is almost twice the one observed on the front face ($D_{\text{Spall Front}} \approx 5\text{-}6\text{mm}$). Even if we observed a small increase, these dimensions seem not very sensitive to the impacting velocity. Figure 6 illustrates the damages observed on a DDS, the shattered zone is limited to close hole's periphery whereas the spall zone extends to a much larger surface.

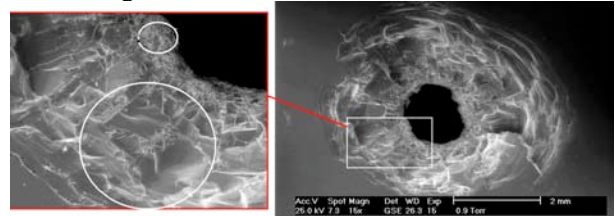


Figure 6 SEM view of a DDS impacted by MICA at 3.2 km/s. The picture shows the different damage zones: the perforation hole, the compacted zone and the spall zone

Some interesting samples were also analysed with a confocal microscope to determine their profile after impact (figure 7) and to calculate the total volume ejected during the impact. To illustrate this, for an impact of a 4mg steel projectile at 2.5 km/s on a 2mm DDS the computed ejected mass is 67mg. 85% of this mass is due to rear spallation. In terms of ejected volume more valuable for the debris threat, the ejected volume is around 60 times bigger than the impacting volume. No evidence of projectile residue has been found on the impacted samples even in non perforating cases.

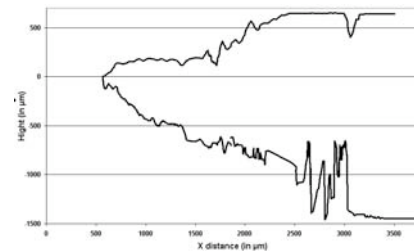


Figure 7 Confocal measurement of a DDS profile after impact. This was used to calculate the ejected volume.

3. EXPERIMENTAL CHARACTERISATION OF EJECTED MATTER

As it has been presented in introduction, the main threat for the space environment as well as for optics of the LMJ experiment chamber is the material ejection due to HVI on thick and thin brittle targets. Not many data on material ejection involving brittle targets are available in literature. ONERA/DESP has been working since the 90's and has identified front face ejection tendencies occurring during HVI on brittle targets but few experimental tests were devoted to this phenomenon. Since 2004, CEA has concentrated part of its work with MICA launcher to characterise material ejection during HVI on 2mm DDS. Two main collection setups were used and will be presented in this part: simple light paperboard coated with adhesive were placed in MICA chamber behind and around the DDS and aerogel collectors were designed to collect fragments ejected at the rear face of the DDS.

3.1. Secondary impacts and collected fragments

Light paperboard (PB) coated with adhesive is an excellent and cost effective fragments collector. For this reason, many paperboard plates were disposed around and behind the impacted DDS. Figure 8 is a SEM view of a PB located 25mm behind a perforated DDS at 2.5km/s.

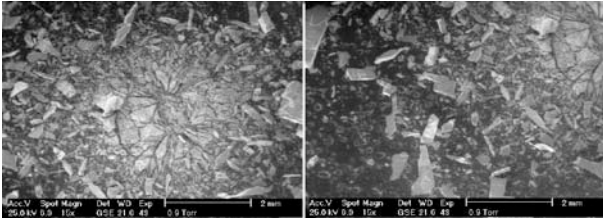


Figure 8 Fragments collected on paperboard located behind the perforated DDS impacted by MICA

As it can be seen on the figure many large fragments were generated by the impact. Three main areas have been identified: a 3 mm in diameter central area showing spalls probably deteriorated during the secondary impact on the paperboard, a peripheral zone made of micro fragments (typical size = 10–50 μm) extends up to 5mm in diameter and a third wide zone extending up to 6.5mm from impact axis is made of long parallelepiped fragments whose typical dimensions are 1x0.1x0.1mm. Relating these different fragments category to their supposed origin and to damages observed on the corresponding DDS is not an easy task. We can nevertheless make some hypothesis: the micro fragments seem to correspond in size with those observed on DDS and may result from fragmentation of fused silica during shock loading. The long parallelepiped fragments probably originate from spallation observed on the rear face of impacted samples. In some cases, similar non-ejected fragments were observed on DDS. The origin of the central area is more difficult to identify because fragments have been probably deteriorated and no projectile residue have been found. The most supposed origin is an important central spallation occurring at the DDS rear face. Knowing the distance from the paperboard to the DDS, diameters of these areas have been used to determine the ejecta clouds geometry: central spall and micro fragments have quasi normal ejection angle (respectively 3.6° and 5.9° from the shooting axis) and parallelepiped fragments have an ejection angle lower than 15°. The reader must notice that these results are consistent with order of magnitude given by ONERA's environmental model.

According to the results presented above, light paperboards appear to be interesting collection diagnostics and allow determining ejection clouds geometry. But fragmentation during secondary impact makes them limited for swift shrapnel. This observation incites the authors to investigate the use of aerogels as shrapnel collectors.

3.2. About the use of aerogels

With the sight of performances of aerogels in terms of hypervelocity particles collection (cf. MEEP experiment), the use of such materials appears to be an excellent way to characterise matter ejection during HVI on brittle target. Numerous cylindrical aerogel blocks were manufactured by the french company

PrimeVerre. Blocks were 20mm high and 60mm in diameter; their density was 0.1 g/cm³. These samples were sized with the clouds geometry calculated above. Left picture of figure 9 shows an aerogel block in its box as it has been integrated into MICA experiment chamber. The right picture is a back-lit view of fragments collected in the aerogel after a 3 km/s impact on a 2mm DDS. Aerogel collectors have proved their ability to collect “intact” high velocity fragments. Analysing silica aerogel and localising silica fragments in it are challenging tasks. At the time of this paper, optical observation was the only method used but many options are being studied. Thus X-ray radiographies may provide precise tomography of the sample allowing locating collected particles. As it can be seen on the picture shrapnel's depth of penetration ranges from 2 mm to 6 mm which are values less than those expected by analytical models or those found in the literature. Many effects can explain this: either the ejection velocity has been overestimated by numerical simulation, either shape effects are prevalent or penetration analytical model are not adequate in these cases. Aerogels are nevertheless new promising collection systems which could give 3D topology of the matter ejected from both faces of the target especially for very high impact velocities. This collection setup will continue to be used on MICA launcher.

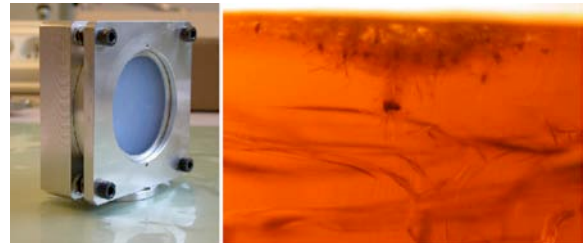


Figure 9 Aerogel collector used on MICA launcher (left) and collected ejecta and spalls (right)

4. NUMERICAL MODELLING OF HVI ON THIN BRITTLE TARGETS WITH LS-DYNA

4.1. Smooth Particle Hydrodynamics method

Smoothed Particle Hydrodynamics (SPH) method is a grid less Lagrangian technique that originated in 1977. The main advantage of the method is to bypass the requirement for a numerical grid to calculate spatial derivatives. This avoids the severe problems associated with mesh tangling and distortion which usually occur in Lagrangian analyses involving large deformations. SPH uses a kernel approximation which is based on interpolation points with no assumptions about which points are neighbours to calculate spatial derivatives. To illustrate this, let consider a continuum represented by a set of interacting particles, as shown in figure 10. Each particle I interacts with all other particles J that are within a given distance $2h$ from it. The distance h is called the smoothing length. The interaction is weighted by the function $W(x_i-x_j,h)$ which is called the smoothing (or kernel) function. Using this principal, the value of a continuous function, or its derivative, can be estimated at any particle i based on known values at the surrounding particles j at each time using the following kernel estimates:

$$\langle f(x_i) \rangle \approx \int f(x_j) W(x_i - x_j, h) dx_j \quad (1)$$

where f is a function of the three dimensional position vector x_i , dx_j is a volume and W , the smoothing function (commonly the cubic B-spline).

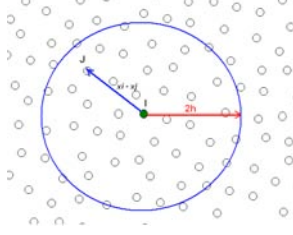


Figure 10 Neighbouring particle geometry for SPH methodology in Ls-Dyna

After several steps of derivation and by converting the continuous volume integrals to sums over discrete interpolation points, the equations of conservation governing the evolution of mechanical variables on each particle can be expressed as follow:

$$\frac{d\rho}{dt}(x_i) = -\rho \cdot \text{div}(v(x_i)) = \sum_{j=1}^N m_j (v(x_j) - v(x_i)) A_{ij} \quad (2)$$

$$\frac{dv^\alpha}{dt}(x_i(t)) = \frac{1}{\rho_i} \frac{\partial(\sigma^{\alpha\beta})}{\partial x_i}(x_i(t)) = \sum_{j=1}^N m_j \left(\frac{\sigma^{\alpha\beta}(x_j)}{\rho_j^2} A_{ij} - \frac{\sigma^{\alpha\beta}(x_i)}{\rho_i^2} \right) A_{ji} \quad (3)$$

$$\frac{dE}{dt}(x_i) = -\frac{P}{\rho} \nabla v(x_i) = -\frac{P_i}{\rho_i^2} \sum_{j=1}^N m_j (v(x_j) - v(x_i)) A_{ij} \quad (4)$$

where x_i is the spatial coordinate of particle i .

The calculation cycle is similar to that for a lagrangian computation except for the steps where a kernel approximation is used. Kernel approximations are used to compute forces from spatial derivatives of stress and spatial derivatives of velocity are required to compute strain rates.

4.2. Johnson Holmquist 2 material model

Johnson and Holmquist have presented two closely related constitutive models for brittle materials. The calculations presented in this study were obtained using the JH2. The model includes a representation of the intact and fractured strength, a pressure to volume relationship (equation of state) that can include bulking and a damage model that transitions the material from an intact state to a fractured state. The normalised equivalent stress for the strength is given by:

$$\sigma^* = \sigma_i^* - D(\sigma_i^* - \sigma_f^*) \quad (5)$$

where $\sigma^* = \frac{\sigma}{\sigma_{HEL}}$, σ_{HEL} is the equivalent stress at the Hugoniot elastic limit (HEL), D is the damage ($0 < D < 1$), σ_i^* is the normalised intact strength and σ_f^* is the normalised fractured strength. These strengths can be written as follow:

$$\sigma_i^* = A(P^* + T^*)^N (1 + C \ln \dot{\epsilon}^*) \leq \sigma_{i \max}^* \quad (6)$$

$$\sigma_f^* = B(P^*)^M (1 + C \ln \dot{\epsilon}^*) \leq \sigma_{f \max}^* \quad (7)$$

with $T^* = \frac{T}{P_{HEL}}$; $P^* = \frac{P}{P_{HEL}}$ and $\dot{\epsilon}^* = \frac{\dot{\epsilon}}{\dot{\epsilon}_0}$ with $\dot{\epsilon}_0 = 1s^{-1}$

which are respectively the normalised maximum tensile pressure, the normalised pressure and the dimensionless strain rate. The material constants are A, B, C, M, N, T

and $\sigma_{f \max}^*$. The hydrostatic pressure before fracture is calculated using a polynomial equation of state. The bulking effect is included by adding an incremental pressure P .

To simulate the rupture, particles are deactivated at a pressure cut-off ($P = -150\text{MPa}$). This way of creating discontinuities is the most effective as it has been reported by (Mandel et al, 1996). All the results presented below use a JH2 set of parameters calibrated on shock experiment realised by Cagnoux (1985) on Pyrex glass and on data of the material model used at CEA-CESTA for fused Silica that are confidential.

4.3. Numerical simulations of HVI on EPA

The calculations presented in this section concern normal hypervelocity impacts involving steel projectiles on 2mm thick DDS at velocities ranging from 1 to 4 km/s. A quarter 3D model has been built to decrease computational time and uses two sph symmetry planes. In order to mesh the plate with an efficient way, we have divided it into two parts with different mesh densities: a total of about 210.000 particles were used.

Damages caused by impacts on DDS: Validation

Ls-Dyna/SPH and JH2 model provide very good results: damage characteristics presented in section 2 (front and rear spalls, perforation hole) are also present in the simulation results as shown on fig 12 where fig 8 has been superimposed. The velocity at the ballistic limit for a 500 μm diameter steel projectile is around 1500m/s; this value is consistent with samples analysis impacted by MICA. Figure 11 and table 1 compare results of both numerical calculations and sample analysis. The relative importance of front and rear spallation are consistent with confocal measurements in terms of height of the spallation zones (800 μm /1200 μm) and in terms of relative diameters of spall area ($D_{\text{SpallFront}}/D_{\text{SpallBack}} = 0.6$ in calculations and sample analysis for an impact at 3 km/s). When looking at maximal spall diameter values, the difference between numerical model and sample analysis is more important but the existence of very thin spalls at the periphery of the crater increases the damaged diameter without increasing too much the ejected volume.

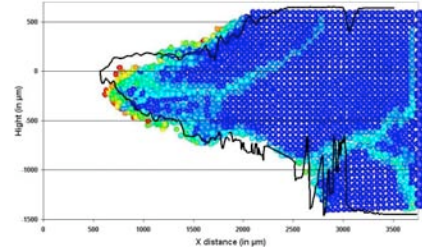


Figure 11 Comparison of profiles obtained with Ls-Dyna and after sample analysis (black curve) showing the good accordance between both results.

Table 1 Comparison of experimental and numerical damages seen by DDS during an impact at 3 km/s.

Data in mm	Hole	Front Face Damages		Rear face Damages	
	D_h	$D_{\text{SpallFront}}$	$H_{\text{SpallFront}}$	$D_{\text{SpallBack}}$	$H_{\text{SpallBack}}$
Shot 01-05	2.35	5.7	800 μm	9-10	1.2
LsDyna/sph	2.14	4.9	840 μm	6.5-8.1	1.16

Numerical modelisation of matter ejection during HVI on DDS

The readers must notice that the authors have extrapolated particles clusters as fragments. The clusters results from contact loss between particles mainly due to desactivation of border particles. Identifying discontinuities and rupture criteria is a challenging task in sph and this is part of ongoing research activities at ENSICA/DGM. In the case of a 3km/s impact on a 2mm DDS, three types of them can be identified: ejecta, micro spalls and macro spalls. Ejecta consist of isolated and/or totally fractured particles ($\varnothing < 50\mu\text{m}$). Their ejection velocities range from 250 to 1000 m/s for a 3km/s impact. Micro and macro spalls families consist of particles clusters of different sizes (cf. figure 12): the micro spalls are typically $400 \times 400 \times 100\mu\text{m}$ fragments whereas macro spalls are typically $1500 \times 1000 \times 60\mu\text{m}$ spalls. Their ejection velocities range respectively from 60 to 120 m/s for micro spalls and from 15 to 40 m/s for macro spalls. All these fragments are present on both face of the DDS. In terms of clouds geometry, a conical cloud is observed on the front face during the first 10 μs of the simulation then the spalls are ejected perpendicularly the main plane of the DDS: their angle of ejection from the normal of the DDS range from -5° to $+5^\circ$. On the rear face of the DDS, ejecta are ejected along the normal of the DDS ($< 5^\circ$) and spalls have ejection angles ranging from 5° to 15° . All these resultants are consistent with the analysis of the paperboard collector (cf. part 3.) and with ONERA environmental model (Bariteau, Mandeville, 2001).

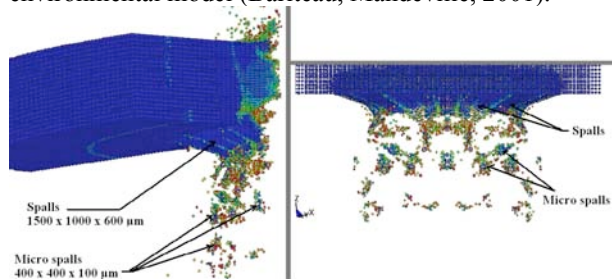


Figure 12 Extrapolation of particles clusters as fragments : 2 types of spalls can be identified, macro and micro spalls.

For a velocity range of 2 to 4 km/s, the main effect of the velocity was the fragments velocity but no important effects have been observed on clouds geometry.

5. CONCLUSIONS AND PROSPECTS

This article presents the work resulting from collaboration between four organisms involved in hypervelocity impacts for two different strategies. Both of concerned activities worry about material ejection during HVI on brittle targets. This collaboration leads to the construction of an important database on damages seen by brittle targets during hypervelocity impacts at various velocities, scales and angle of incidence of the projectile. The case of thin brittle targets has been highlighted as the most critical for the space environment because all damages and particularly spallation occurs on both faces of the target. Rear spallation is indeed more important than front spallation and represents more than 80% of the total ejected mass for velocities above 1.5km/s. These remarks motivated the authors to assess damages and matter ejection in simple thin SiO₂ targets before considering complex

multilayered structures like solar cells. Experimental techniques have been used to collect and characterise matter ejection occurring during HVI on thin brittle targets. The use of silica aerogel as laboratory collector is a very promising technique for determining ejection velocities. These collection setups allow determining types of ejected fragments and general tendencies of rear matter ejection. In this paper, the authors have also shown the capabilities of the Ls-Dyna mesh free SPH method coupled with the JH2 material model. Simulations of HVI on 2mm thin brittle plates at velocities ranging from 1 to 4 km/s give results that are in good correlation in terms of damages let in the target: perforation hole and spallation zones were reproduced with very satisfying results. In terms of matter ejection, numerical simulations appear to predict in a satisfactory way ejection velocities and corresponding fragments. Difficulties in identifying clusters of particles as fragments comfort the authors to improve material model criteria and the sph method especially for spallation and creation of discontinuities. Our future work will consist in experimentations of oblique impacts (CEA-CESTA) with corresponding numerical simulations and ejecta/spalls collection. Higher velocity (6-8km/s) on DDS are also planned and fragments collection on both faces of the target using aerogel will be carry on for all these experiments. With the sight of space applications, numerical simulations of HVI on Hubble solar cells is being performed at ENSICA using JH2 material model and Ls-Dyna SPH method. These simulations will be compared with cells analysis performed by ONERA.

6. ACKNOWLEDGEMENTS

The authors would like to thanks Laurent Duffours (PrimeVerre) for manufacturing aerogels collectors and for his advice during experimentations and Michel Labarrère and Daniel Boitel (ENSICA) for their help during samples analysis.

7. REFERENCES

- M. Bariteau, J.C. Mandeville, A modelling of ejecta as a space debris source, ESOC, Darmstadt, Germany, 19-21 March 2001, ESA SP-473, October 2001
- M Bariteau, Prolifération des débris orbitaux : production et évolution des particules secondaires, *Thèse de l'Ecole Nationale Supérieure de l'Aéronautique et de l'Espace, 2001*
- J. Cagnoux, Déformation et ruine d'un verre pyrex soumis à un choc intense, these de l'université de Poitiers, 1985.
- J.L. Lacome, Smoothed particles hydrodynamics – Part I and II, Livermore Software Technology Corporation, 2001.
- Mandell D.A., Wingate C.A., and Schwalbe L.A., Simulation of a ceramic impact experiment using the SPHINX SPH code, 16th International Symposium on ballistics, San Francisco, CA, 1996.
- A. Moussi, J.C. Mandeville, Oblique HVI: implication for the analysis of material retrieved after exposure to space, To be published in HVIS 2005.
- M Rival, HVI de micrométéorites et débris orbitaux sur les satellites, *Thèse de l'Ecole Nationale Supérieure de l'Aéronautique et de l'Espace, 1997*